

Effect of superficial velocity on liquid injectivity in SAG foam EOR. Part 1

Experimental study

Gong, Jiakun; Flores Martinez, Wendy; Vincent-Bonnieu, Sebastien; Kamarul Bahrim, Ridhwan Zhafri; Che Mamat, Che A.Nasser Bakri; Tewari, Raj Deo; Mahamad Amir, Mohammad Iqbal; Farajzadeh, Rouhollah; Rossen, William

DOI

[10.1016/j.fuel.2020.118299](https://doi.org/10.1016/j.fuel.2020.118299)

Publication date

2020

Document Version

Final published version

Published in

Fuel

Citation (APA)

Gong, J., Flores Martinez, W., Vincent-Bonnieu, S., Kamarul Bahrim, R. Z., Che Mamat, C. A. N. B., Tewari, R. D., Mahamad Amir, M. I., Farajzadeh, R., & Rossen, W. (2020). Effect of superficial velocity on liquid injectivity in SAG foam EOR. Part 1: Experimental study. *Fuel*, 278, Article 118299. <https://doi.org/10.1016/j.fuel.2020.118299>

Important note

To cite this publication, please use the final published version (if applicable).
Please check the document version above.

Copyright

Other than for strictly personal use, it is not permitted to download, forward or distribute the text or part of it, without the consent of the author(s) and/or copyright holder(s), unless the work is under an open content license such as Creative Commons.

Takedown policy

Please contact us and provide details if you believe this document breaches copyrights.
We will remove access to the work immediately and investigate your claim.



Full Length Article

Effect of superficial velocity on liquid injectivity in SAG foam EOR. Part 1: Experimental study



Jiakun Gong^{a,*}, Wendy Flores Martinez^a, Sebastien Vincent-Bonnieu^{a,b},
 Ridhwan Zhafri Kamarul Bahrim^c, Che A Nasser Bakri Che Mamat^c, Raj Deo Tewari^c,
 Mohammad Iqbal Mahamad Amir^c, Rouhollah Farajzadeh^{a,b}, William Rossen^a

^a Department of Geoscience and Engineering, Delft University of Technology, 2628 CN Delft, The Netherlands

^b Shell Global Solutions International B.V., 1031 HW Amsterdam, The Netherlands

^c PETRONAS, Kuala Lumpur 50088, Malaysia

ARTICLE INFO

Keywords:

Foam
 Enhanced-oil-recovery
 Surfactant-alternating-gas
 Injectivity
 Superficial velocity
 Shear thinning

ABSTRACT

Surfactant-alternating-gas (SAG) is a preferred method of foam injection, which is a promising means of enhanced oil recovery. Liquid injectivity in a SAG process is commonly problematic. Our previous studies suggest that the liquid injectivity can be better than expected due to the existence of a collapsed-foam region formed during the gas-injection period ahead of the liquid-injection period. A single superficial velocity was used in those studies to examine the flow behavior during gas- and liquid-injection periods, separately. However, in radial flow from an injection well, superficial velocity decreases with distance from the injection well. Understanding the effect of superficial velocity on gas and liquid injectivities is important, but remains unexplored. In this study, we first examine gas injection at different superficial velocities following foam injection. We then study the effect of liquid superficial velocity on the liquid injectivity following a similar volume of gas injection. Our results show that during a prolonged period of gas injection following foam, the propagation velocity and the total mobility of the collapsed-foam bank are not significantly affected by the gas superficial velocity. During liquid injection after a period of gas injection, the dimensionless propagation velocities and the total mobilities of the forced-imbibition bank and the gas-dissolution bank follow a power-law dependence on the liquid superficial velocity. Liquid fingering through the weakened-foam region shows strongly shear-thinning behavior. It is also observed from X-ray computer-tomography experiments that the liquid fingers are wider if the liquid superficial velocity is greater. The impact of the shear-thinning behavior on the estimation of liquid injectivity in a field application is the subject of a companion paper.

1. Introduction

Foam is a well-known method for enhanced oil recovery, due to its capability for improving gas sweep efficiency [1–3]. There are two main foam-injection strategies: co-injection of gas and surfactant solution, and injecting gas and surfactant solution alternatively. Surfactant-alternating-gas (SAG) injection [4,5] is a favored method for foam injection into a formation because of the excellent gas injectivity and the reduced risk of facility-corrosion issues [6]. However, a SAG process often suffers from poor liquid injectivity. The pressure rise at the injection well can be great, in turn fracturing the well [7,8]. Several studies have been performed for liquid injectivity directly after steady-state foam injection [9–16]. Liquid injectivity following full-strength foam is very poor.

In our previous study, we examined liquid injectivity after a period of gas injection, as in a SAG process [16]. We found that a period of gas injection significantly affects the subsequent liquid injectivity in a SAG process [16]. During the gas-injection period, a collapsed-foam region forms near the injection face, in which foam completely collapses or greatly weakens, leaving a limited amount of trapped gas. The collapsed-foam region slowly propagates downstream. During subsequent liquid injection, liquid first quickly imbibes into the collapsed-foam region, and then fingers through the trapped foam further downstream. Various banks are observed in our coreflood experiments. During the gas-injection period, the core is occupied by the collapsed-foam bank and the weakened-foam bank. During the subsequent liquid-injection period, the collapsed-foam bank, the forced-imbibition bank and the gas-dissolution bank are observed. These banks are not represented in

* Corresponding author.

E-mail address: j.gong@tudelft.nl (J. Gong).

<https://doi.org/10.1016/j.fuel.2020.118299>

Received 12 October 2019; Received in revised form 30 May 2020; Accepted 2 June 2020

0016-2361/ © 2020 The Authors. Published by Elsevier Ltd. This is an open access article under the CC BY license (<http://creativecommons.org/licenses/by/4.0/>).

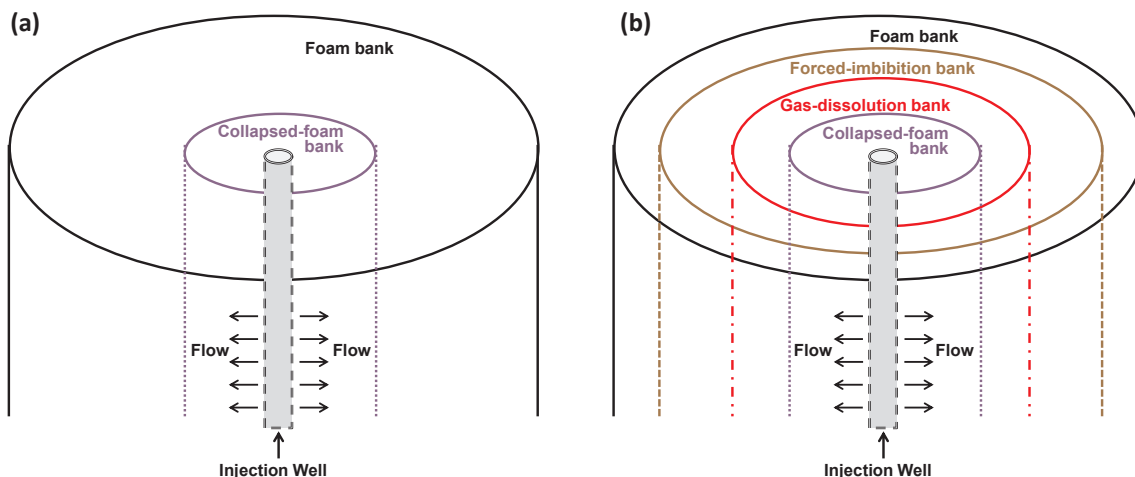


Fig. 1. Banks observed in SAG-foam coreflood experiments applied to radial flow around an injection well. (a) Banks during the gas-injection period. (b) Banks during the liquid-injection period.

current foam simulators [17]. If the core-scale behavior is scaled up to radial flow in the field, the near-well region is then occupied by various banks as shown in Fig. 1. In our previous studies [16,17], the forced-imbibition bank was called liquid-fingering bank.

In our previous work, gas and liquid slugs were each injected at one superficial velocity. However, in radial flow around an injection well, the superficial velocity changes with the radius. It is important to understand the flow behavior at various superficial velocities during the gas- and liquid-injection periods, which could have strong impact on injectivity in a SAG process.

In this study, we examine the flow behavior during gas and liquid injection in a SAG process at various superficial velocities. CT scanning is applied to help understand the difference in the flow phenomena during liquid injection at relative low and high superficial velocities.

2. Experimental methods

2.1. Materials

The coreflood experiments are conducted with a Berea sandstone core sample. The core is 17-cm long, with a 3.8-cm diameter. The measured average permeability of the core is 160 mD and the measured average porosity is 0.2. The permeability is calculated from the pressure gradients during liquid (brine) flow through the core at various flow rates. The porosity is determined from the CT measurements.

Surfactant solution with concentration of 0.5 wt% is prepared by mixing synthetic brine and AOS C14-16 surfactant. The synthetic brine (3 wt% salinity) contains five salts, i.e. sodium chloride (1.84 wt%), magnesium chloride (0.73 wt%), sodium sulphate (0.28 wt%), calcium chloride (0.1 wt%) and potassium chloride (0.05 wt%) [16]. Nitrogen gas with 99.99% purity is supplied from a gas cylinder.

2.2. Experimental setup

Fig. 2 schematically shows the experimental apparatus. The 17-cm-long Berea core is built into a core holder and placed vertically inside an oven in order to maintain the experimental temperature at 90 °C. Pressure drop is measured across five sections. The inlet and outlet sections are both 2.2 cm long, and the three middle sections are each 4.2 cm long. To avoid the entry effect and the capillary-end effect, we only study the three middle sections, i.e. Sec. 2 – 4 in the schematic (Fig. 2). Gas and surfactant solution are injected from the bottom of the core to minimize the effect of gravity override. They are either co-injected to generate steady-state foam or injected alternatively to study SAG processes. The injection velocities of gas and surfactant solution

are controlled by a mass-flow controller and a liquid pump, respectively. All experiments are conducted with a 40-bar back pressure.

We also repeat two experiments supplemented with X-ray computer-tomography measurements to relate the water saturation to the pressure gradient. In the CT-scan experiments, the oven is replaced by an electric heating jacket to maintain the core temperature at 90 °C. The core is placed horizontally. The pressure gradients are comparable to the corresponding experiments with the core placed vertically. A third-generation Siemens Somatom CT scanner is used.

2.3. Experimental procedure

The same Berea core is used for all experiments except the CT-scan experiments. In the CT-scan experiments, a similar core from the same block (measured average permeability 160 mD, and measured average porosity 0.2) is used. In each experiment, we first generate state-state foam in the core by co-injecting nitrogen and surfactant solution. After each experiment, the core is restored to remove trapped gas by flushing it with 10 PV of cleaning solution (50% isopropanol and 50% tap water) followed by 20 PV of tap water, and then CO₂ is injected to displace the remaining gas, finally vacuuming before re-saturating the core with brine. The permeability is measured each time to ensure the core is under a similar initial condition.

We first examine the effect of gas-slug size on subsequent liquid injection, especially the length of the plateau in pressure gradient. We then study the effects of gas and liquid superficial velocities on flow behavior during the gas- and liquid-injection periods, respectively. We also study the effect of initial foam quality (gas fractional flow), i.e. 0.6-quality foam (low-quality regime) and 0.95-quality foam (high-quality foam) on the liquid-injection period. The foam quality is the value at the outlet of the core. CT scanning is applied in two experiments to visualize the flow behavior when liquid is injected at a relative low superficial velocity (2 ft/day) and high superficial velocity (200 ft/day) after a similar amount of gas injection. The sequence of experiments are summarized in Table 1.

3. Results

3.1. Effect of gas-slug size on liquid flow in weakened-foam bank

In our previous work [16], we show that liquid injectivity is strongly affected by the period of gas injection ahead of it. The larger the amount of gas injected, the bigger the collapsed-foam bank created. Liquid then quickly fills the collapsed-foam bank, and then more slowly fingers through the weakened-foam bank. In this study, we conduct a

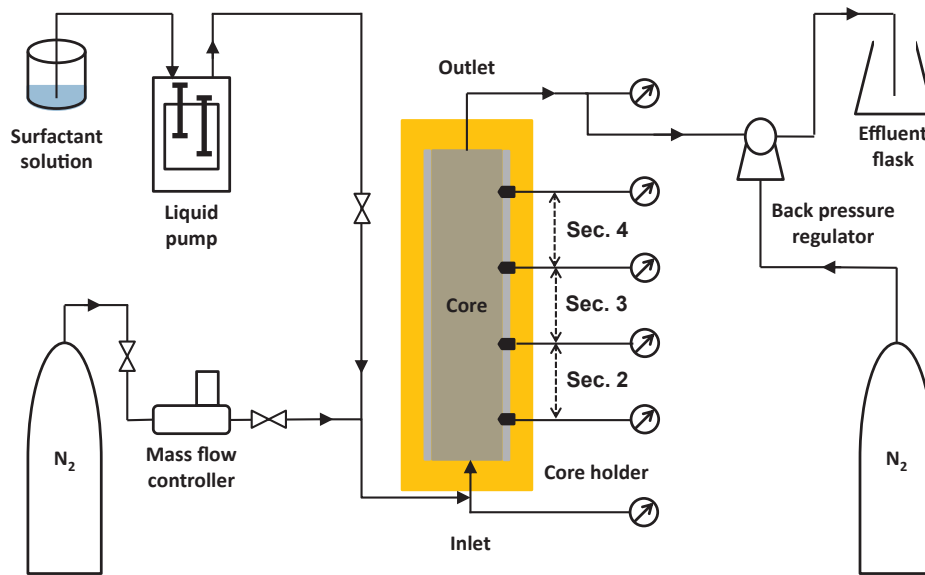


Fig. 2. Schematic of experimental apparatus.

series of coreflood experiments to investigate the impact of the previous period of gas injection on liquid flow in the weakened-foam bank. In all the cases, 0.95-quality steady-state foam is injected initially. Various amounts of gas are then injected before the liquid slug, ranging from about 7.5 PV to about 150 PV. Finally, liquid is injected at a superficial velocity of about 2 ft/day (7.06×10^{-6} m/s). Since we aim to study the flow behavior in the weakened-foam region (the region beyond the collapsed-foam region), we study only the pressure gradients in Section 4, which is beyond of the collapsed-foam bank even after about 150 PV gas injection (Fig. 3).

As shown in Fig. 3, the plateau in pressure gradient during liquid injection following about 7.5 PV gas injection lasts roughly 5 PV, and the period increases gradually to about 9 PV for liquid injection following about 150 PV gas injection. This suggests that the larger gas slug injected, the longer that pressure gradient holds nearly constant during subsequent liquid injection. However, the plateau values are not strongly affected by the amount of gas injected, as long as the collapsed-foam bank has not penetrated the region of interest. There are some possible reasons for this phenomenon. After liquid fills the collapsed-foam bank, liquid quickly imbibes into the trapped foam further downstream, establishing a plateau in pressure gradient. Unsaturated

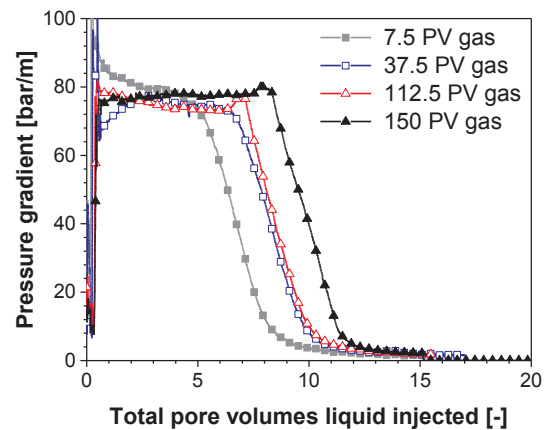


Fig. 3. Pressure gradient in Section 4 during liquid injection following various volumes of gas injection. The core is initially saturated with steady-state foam ($f_g = 0.95$).

Table 1
Summary of core-flood experiments.

Run	Initial foam quality	Gas injection		Liquid injection		Purpose
		Superficial velocity [ft/day]	Amount [PV]	Superficial velocity [ft/day]	Amount [PV]	
1	0.95	6	7.5	2	17	Effect of gas-slug size on subsequent liquid-injection period (Run 1–4)
2	0.95	6	37.5	2	17	
3	0.95	6	112.5	2	17	
4	0.95	6	150	2	26	
5	0.6	3	305	–	–	Effect of initial foam quality on subsequent gas-injection period (Run 5–6)
6	0.95	3	360	–	–	
7	0.95	3	360	–	–	
8	0.95	6	242	–	–	Effect of gas superficial velocity on collapsed-foam region (Run 7–9)
9	0.95	9	320	–	–	
10	0.95	6	150	20	34	
11	0.95	6	150	80	69	Effect of initial foam quality and liquid superficial velocity on liquid injectivity (Run 10–14)
12	0.95	6	150	200	68	
13	0.6	6	150	2	15	
14	0.6	6	150	200	73	Experiments supplemented with CT scan (Run 15–16)
15	0.95	6	150	2	20	
16	0.95	6	150	200	70	

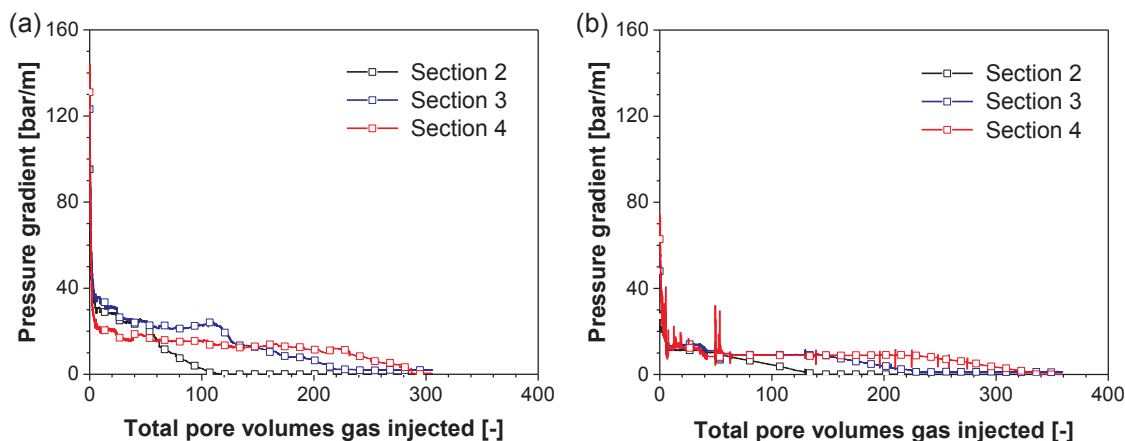


Fig. 4. Pressure gradient during gas injection at 3 ft/day following various qualities of foam. (a) 0.6-quality foam. (b) 0.95-quality foam.

injected liquid then dissolves gas in the collapsed-foam region, an unstable process leading to formation of liquid-saturated fingers taking almost all the liquid flow. The process appears to be similar to formation of wormholes during acid injection into carbonates [18]. Ahead of these fingers, in the forced-imbibition bank, liquid is saturated and no gas is dissolved. The larger the gas slug injected, the larger is the collapsed-foam region formed during gas injection. More liquid becomes saturated in contact with all the gas in the collapsed-foam region. Therefore, the propagation of the front of gas dissolution is delayed, and the plateau in pressure gradient downstream is prolonged.

3.2. Effect of gas superficial velocity

We first investigate the effect of the initial foam quality on the subsequent gas-injection period. Two foam qualities are examined, i.e. $f_g = 0.6$, in the low-quality regime, and $f_g = 0.95$, in the high-quality regime [19,20]. Gas is then injected at 3 ft/day (1.06×10^{-5} m/s) for both cases. As presented in Fig. 4, in both cases, the second decline in pressure gradient propagates in a wave from the inlet to downstream. Take the furthest section of interest (Section 4), for example. The plateau values of the pressure gradients for the two cases are comparable, i.e. about 10 bar/m. The propagation velocities of the collapsed-foam bank are also similar in the two cases; the collapsed-foam bank reaches the end of Section 4 after about 300 PV gas injection for both cases. Therefore, it is reasonable to conclude that there is no strong effect of the initial foam quality on the collapsed-foam bank during the gas-injection period. However, in the very beginning of the gas-injection period, the pressure gradient shoots up to about 150 bar/m with 0.6-quality initial foam, while it is about 75 bar/m for the case with 0.95-

quality initial foam. The flow behavior at the leading edge of the gas deserves further study, however, it is not the focus of this study.

Fig. 5 illustrates the effect of the gas superficial velocity on gas injectivity and the propagation of the collapsed-foam bank. Three superficial velocities are examined: 3 ft/day, 6 ft/day and 9 ft/day (1.06×10^{-5} , 2.12×10^{-5} and 3.18×10^{-5} m/s). The pressure gradients are shown in terms of local pore volume (LPV) in order to show the dimensionless propagation velocity of the collapsed-foam bank more clearly. As defined in our previous work [16], the local pore volume (LPV) is defined as the volume injected (PV injected) divided by the cumulative pore volume from a given position back to the inlet (PV in place). The front of a bank is thus propagates with a dimensionless velocity defined as (PV in place)/(PV injected).

For both Sections 3 and 4, the plateau values in pressure gradient change from 10 bar/m to

20 bar/m as the gas superficial velocity increases from 3 to 9 ft/day. The plateau value in pressure gradient is affected by the gas superficial velocity. Since our main interest lies in the effect of a period of gas injection on the subsequent liquid injectivity in a SAG process, we care more about the effect of the gas superficial velocity on the collapsed-foam bank. As shown in Fig. 5, the pressure gradient becomes very small after a prolonged period of gas injection, which indicates foam collapse or great weakening. The total mobility ($\nabla p/u_t$) of a bank is calculated from the pressure gradient (∇p) and the total superficial velocity (u_t) based on Darcy's Law (approximating foam flow as single phase-flow). As presented in Fig. 5, the total mobility of the collapsed-foam bank is not significantly affected by the superficial velocity during gas injection.

The collapsed-foam bank arrives at the end of Sections 3 and 4 after

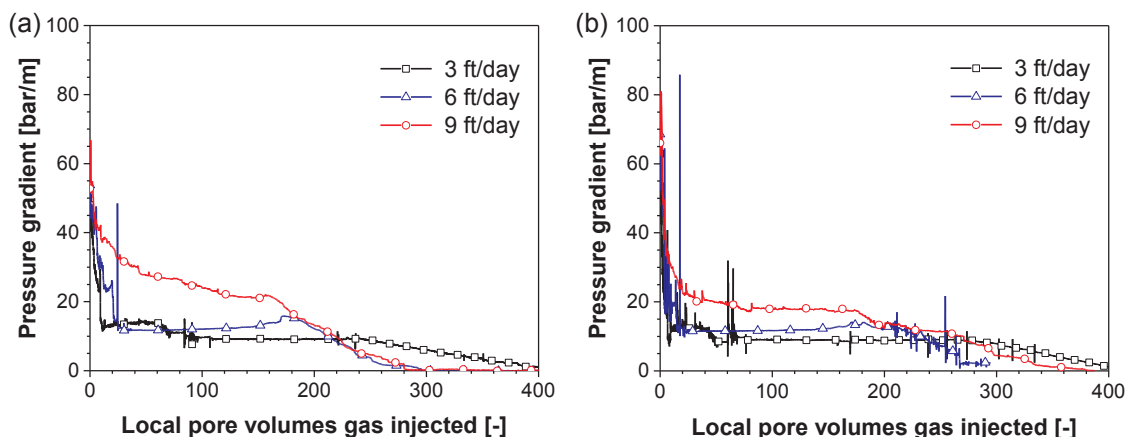


Fig. 5. Propagation of the collapsed-foam bank during gas injection at various superficial velocities. (a) Section 3, (b) Section 4.

Table 2
Properties of the various banks during gas-injection period in a SAG process.

Bank	Superficial velocity [ft/day]	Dimensionless velocity [-]	Total mobility [m ² /Pa*s]
Collapsed-foam Bank	3	2.80×10^{-3}	4.69×10^{-9}
Collapsed-foam Bank	6	1.80×10^{-3}	3.52×10^{-9}
Collapsed-foam Bank	9	2.30×10^{-3}	4.22×10^{-9}
Foam Bank	3	Initially present	1.56×10^{-11}
Foam Bank	6	Initially present	2.34×10^{-11}
Foam Bank	9	Initially present	2.34×10^{-11}

about 300–400 LPV gas injection. In other words, the collapsed-foam bank propagates with a dimensionless velocity between 1/400 and 1/300 for the cases examined. Moreover, there is no consistent trend of the propagation velocity with the gas superficial velocity in Fig. 5. We conclude for simplicity that the collapsed-foam bank propagates with a similar dimensionless velocity for various gas superficial velocities examined, i.e. about 1/350.

The properties of the banks during the gas-injection period in a SAG process at various superficial velocities are summarized in Table 2.

3.3. Effect of liquid superficial velocity

In this section, we present the effect of the liquid superficial velocity on liquid injectivity in a SAG process. We conduct a series of experiments in which surfactant solution is injected at various superficial velocities ranging from 2 ft/day (7.06×10^{-6} m/s) to 200 ft/day (7.06×10^{-4} m/s). In all the experiments, a similar amount of gas (about 150 PV) was injected before liquid injection.

Although gas was injected at the same superficial velocity (6 ft/day) in all these cases, the propagation velocities of the collapsed-foam bank may not be exactly the same in each case, and therefore the collapsed-foam bank may not reach the same position for different cases. The total mobility and the dimensionless propagation velocity of liquid flowing in the collapsed-foam bank are not significantly affected by the superficial velocity of liquid. Here we focus on the flow behavior in the section of the core where foam still remains after a period of gas injection: specifically, Section 4, which is beyond the collapsed-foam bank in all the experiments.

As presented in Fig. 6, liquid injection at both low (2 ft/day) and high (200 ft/day) superficial velocity shows similar overall behavior. The pressure gradient first shoots up to a large value, then holds for a while, and decreases gradually. This suggests that liquid first enters the core with a relative high mobility (the initial low pressure gradient); then liquid disperses across the core cross section. Thereafter, gas dissolution into unsaturated liquid triggers formation of liquid fingers. Liquid then fingers through the trapped gas. The forced-imbibition and

gas-dissolution bank moves as a wave from the inlet towards the outlet, as discussed in our previous work [16]. However, the plateau in pressure gradient for liquid injection at a high superficial velocity (Fig. 6b) is not as obvious as the one for liquid injection at a low superficial velocity (Fig. 6a). It takes a much longer time for the pressure gradient to decrease to the final stage (about 30 PV) for liquid injection at a high superficial velocity (200 ft/day), while it only takes about 2 PV for liquid injection at a low superficial velocity (2 ft/day). In other words, more liquid is needed to dissolve gas at a higher liquid superficial velocity.

In order to understand the difference in flow pattern during liquid injection at low and high superficial velocities in a SAG process, we conduct two CT-scan experiments. The dynamic changes in water saturation are measured and related to mobility changes (Figs. 7-9). About 150 PV gas was injected before the liquid-injection period. Liquid is then injected at either 2 ft/day or 200 ft/day.

Fig. 7 presents the axial water-saturation profile of the middle of the core during liquid injection at 2 ft/day (Fig. 7a) and 200 ft/day (Fig. 7b) after a similar amount of gas injection (150 PV). Initially, when the core is filled with steady-state foam, the water-saturation profiles for the two cases are comparable (top row of the figures). In the second row of the figures, the yellow lines indicate the front of the collapsed-foam bank after a similar amount of gas injection following steady-state foam. As shown in the reconstructed CT images, the collapsed-foam bank arrives at a similar position for the two cases examined. Beyond the collapsed-foam bank, the color at the top of the images is somewhat darker than that of lower places. This implies that foam is drier at the top; however, foam is not collapsed or greatly weakened there according to the pressure gradient. During the liquid-injection period, for both liquid superficial velocities, liquid first quickly imbibes into the collapsed-foam bank. In the weakened-foam region beyond the collapsed-foam region, liquid flows primarily through a liquid finger at the low superficial velocity (2 ft/day). For liquid injection at the high superficial velocity (200 ft/day), liquid flows through the entire cross-section, in spite of the presence of a liquid finger (Fig. 7).

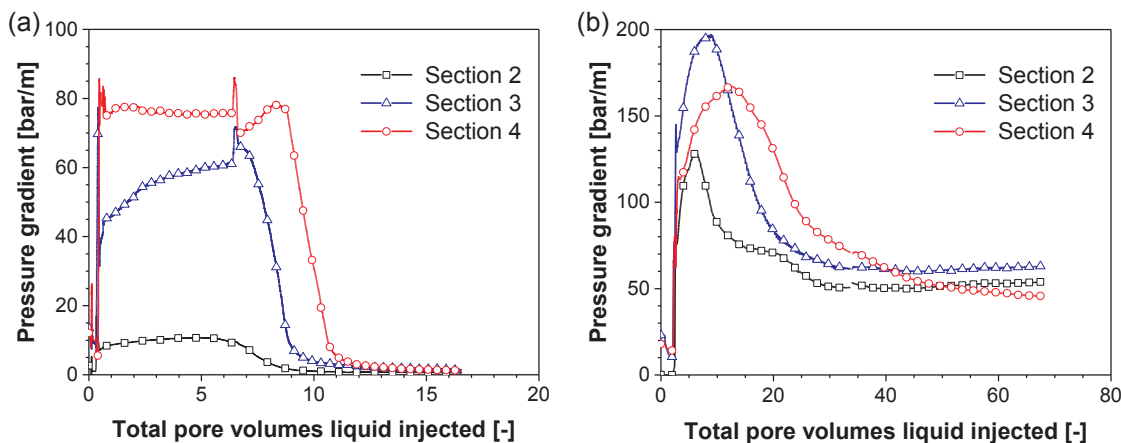


Fig. 6. Pressure gradients during liquid injection at various superficial velocities after a similar amount of gas injection (150 PV). (a) 2 ft/day, (b) 200 ft/day.

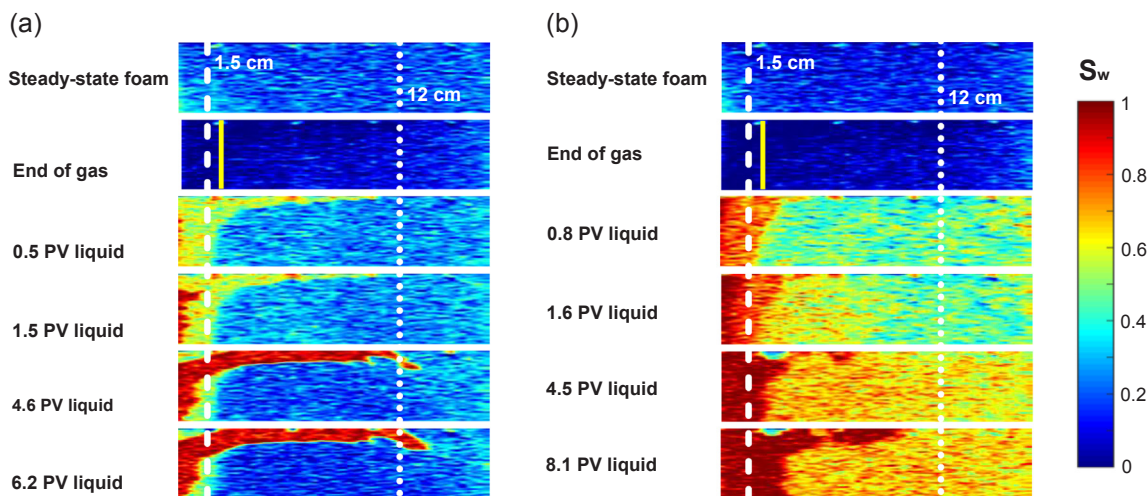


Fig. 7. Vertical water-saturation profile through the axis of the core during liquid injection at various superficial velocities after about 150 PV gas injection. (a) 2 ft/day, (b) 200 ft/day. The yellow lines roughly represent the front of the collapsed-foam bank before liquid injection. White dashed line: position 1.5 cm from inlet. White dotted line: position 12 cm from inlet.

Fig. 8 shows the cross-sectional water-saturation profile at a position (1.5 cm from the inlet) within the collapsed-foam bank. At the low liquid superficial velocity, liquid first sweeps the entire cross section, then a preferential path forms. At the high liquid superficial velocity, liquid imbibes uniformly into the whole cross section. There is no preferential path, illustrated by the nearly-uniform water-saturation distribution. Unsaturated liquid dissolves gas across the whole cross section.

Fig. 9 compares the cross-sectional water-saturation profile at a position (12 cm from the inlet) beyond the collapsed-foam region for liquid injection at the two superficial velocities. At the low superficial velocity (Fig. 9a), liquid sweeps the whole cross section (color changes from dark to light blue) in the beginning. A liquid finger then becomes visible at this position after about 4.6 PV liquid injection, and grows outwards over time. Presumably, nearly all liquid flows through the liquid finger, since the liquid relative permeability would be much greater there. However, at the high superficial velocity (Fig. 9b), no liquid finger is visible after a similar amount of liquid injection, i.e. 4.5 PV. Liquid sweeps the entire cross section. Over time, water saturation increases throughout the cross-section, indicating gas dissolution into unsaturated liquid flowing through the regions. At a greater pressure gradient, liquid is forced into the whole cross-section, not just the finger, and the formation and propagation of the finger is delayed at a

higher superficial velocity. The mechanism may be similar to that of wormhole formation in acidization of carbonates, where acid sweeps more uniformly and fingering is suppressed at a greater superficial velocity [18].

Fig. 10 compares the pressure gradients in the same section (Section 4) during liquid injection at various superficial velocities. The forced-imbibition bank and the gas-dissolution bank show strongly shear-thinning behavior. For the forced-imbibition bank, the plateau value of the pressure gradient rises only about a factor of two as the superficial velocity rises 100 times, from 2 ft/day to 200 ft/day. For the gas-dissolution bank, the shear-thinning behavior is not as strong as for the forced-imbibition bank. However, still, the pressure gradient at the final stage increases only about 30 times when the superficial velocity is 100 times greater.

In the experiments discussed above, the core is always initially saturated with 0.95-quality foam. Fig. 11 shows that the flow behavior during the liquid-injection period in a SAG process is not significantly affected by the initial foam quality, for liquid injection at both the low and high superficial velocities. This suggests that, regardless of the details of the foam state before gas injection (in this case, initial foam quality, in the low- or high-quality regime), foam in the core reaches a similar state after a similar volume of gas injection, as long as the foam is not collapsed or greatly weakened then. A separate study [21] found

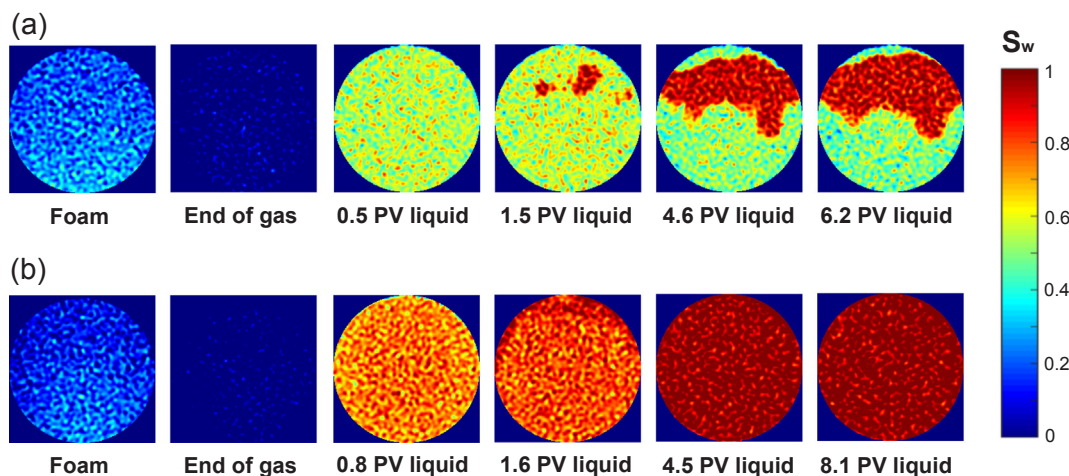


Fig. 8. Cross-sectional water saturation profile at a position 1.5 cm from the inlet (within the collapsed-foam bank) during liquid injection at various superficial velocities. (a) 2 ft/day, (b) 200 ft/day.

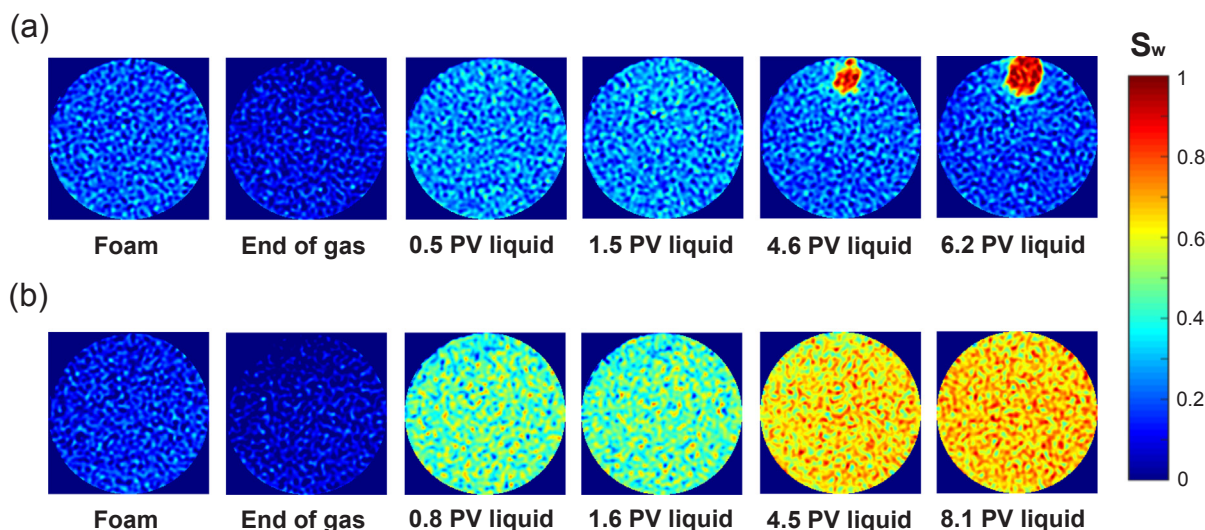


Fig. 9. Cross-sectional water-saturation profile at a position 12 cm from inlet (beyond the collapsed-foam bank) during liquid injection at various superficial velocities. (a) 2 ft/day, (b) 200 ft/day.

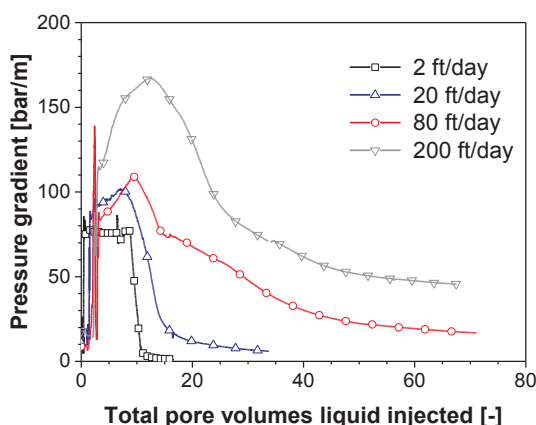


Fig. 10. Pressure gradient in Section 4 (beyond the collapsed-foam region) during liquid injection at various superficial velocities following a similar amount of gas injection (about 150 PV).

that the mobilities and properties of the near-well banks during liquid and gas injection were similar for the first slugs and subsequent slug injection.

The properties of the banks observed during the liquid-injection period at various superficial velocities are summarized in Table 3. The

fitting of the data to the specific values of bank mobilities and propagation velocities is described in our companion paper [22].

4. Concluding remarks

In this work, we investigate the effect of superficial velocities of gas and liquid on the gas- and liquid-injection periods in a SAG process. The experimental findings are summarized as follows:

- In a SAG foam process, the more gas injected before the liquid slug, the longer the plateau in pressure gradient during the liquid-injection period. Beyond the collapsed-foam bank, the plateau in pressure gradient is not strongly affected by the volume of gas injected before the liquid slug.
- During the gas-injection period, the total mobility and the dimensionless propagation velocity of the collapsed-foam bank are not significantly affected by the gas superficial velocity.
- During the liquid-injection period, the flow behavior is strongly affected by the liquid superficial velocity. The forced-imbibition bank and the gas-dissolution bank show strongly shear-thinning behavior. This suggests that reducing injection rate during liquid injection may not reduce the pressure rise at the well as much as might be expected.
- At a low liquid superficial velocity, liquid fingers through the

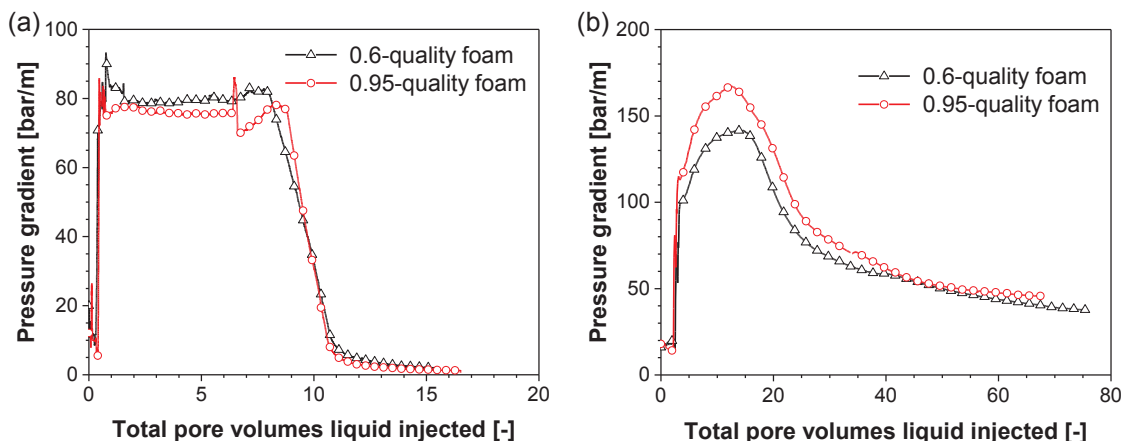


Fig. 11. Pressure gradient in Section 4 during liquid injection after about 150 PV gas injection with different initial foam qualities. (a) 2 ft/day, (b) 200 ft/day.

Table 3
Properties of the various banks during liquid-injection period in a SAG process.

Bank	Superficial velocity [ft/day]	Dimensionless velocity [-]	Total mobility [$\text{m}^2/\text{Pa}\cdot\text{s}$]
Liquid slug in Collapsed-foam Bank	2	0.76	1.46×10^{-10}
Liquid slug in Collapsed-foam Bank	20	0.72	1.82×10^{-10}
Liquid slug in Collapsed-foam Bank	80	0.81	1.95×10^{-10}
Liquid slug in Collapsed-foam Bank	200	0.65	2.70×10^{-10}
Forced-imbibition Bank	2	2.5	8.73×10^{-13}
Forced-imbibition Bank	20	2.08	6.45×10^{-12}
Forced-imbibition Bank	80	1.79	2.43×10^{-11}
Forced-imbibition Bank	200	1.67	4.80×10^{-11}
Gas-dissolution Bank	2	0.078	5.10×10^{-11}
Gas-dissolution Bank	20	0.067	1.02×10^{-10}
Gas-dissolution Bank	80	0.042	1.65×10^{-10}
Gas-dissolution Bank	200	0.035	1.80×10^{-10}

weakened-foam region. However, at a much greater liquid superficial velocity, liquid flows through the entire cross section in spite of the conceptual formation of a big liquid finger.

- The pressure gradient for liquid flowing through the weakened-foam region is not strongly affected by the details of the state of the foam at the start of gas injection (in this case, by initial foam quality). This is true for liquid injection at both low and high superficial velocities.

The implications of these experimental findings to field application are reported in the second part of this work [22].

CRedit authorship contribution statement

Jiakun Gong: Conceptualization, Investigation, Writing - original draft. **Wendy Flores Martinez:** Investigation. **Sebastien Vincent-Bonnieu:** Conceptualization, Formal analysis. **Ridhwan Zhafri Kamarul Bahrim:** Validation, Resources. **Che A Nasser Bakri Che Mamat:** Resources, Project administration. **Raj Deo Tewari:** Resources, Project administration. **Mohammad Iqbal Mahamad Amir:** Validation. **Rouhollah Farajzadeh:** Conceptualization, Formal analysis. **William Rossen:** Conceptualization, Writing - review & editing, Supervision.

Declaration of Competing Interest

The authors declare that they have no known competing financial interests or personal relationships that could have appeared to influence the work reported in this paper.

Acknowledgement

We gratefully thank PETRONAS and Shell Global Solution International B.V. for supporting this work. We also thank the technical support of Michiel Slob and Ellen Meijvogel-de Koning at the Laboratory Geoscience and Engineering of Delft University of Technology.

References

- [1] Kovscek AR, Radke CJ. (1994). Fundamentals of Foam Transport in Porous Media. In *Foams: Fundamentals and Applications in the Petroleum Industry*, Chap. 3, 115-163. Advances in Chemistry, American Chemical Society.
- [2] Rossen WR. (1996). Foams in enhanced oil recovery. In *Prud'homme, R.K., Khan, S. A. (eds.) Foams: Theory, Measurements and Applications*, pp. 413 – 464. Marcel Dekker, New York City.
- [3] Rossen WR, van Duijn CJ, Nguyen QP, Shen C, Vikingstad AK. Injection strategies to overcome gravity segregation in simultaneous gas and water injection into homogeneous reservoirs. *SPE J* 2010;15(1):76–90. <https://doi.org/10.2118/99794-PA>.
- [4] Kibodeaux KR, Rossen WR. Coreflood study of surfactant-alternating-gas foam processes: implications for field design. 1997. <https://doi.org/10.2118/38318-MS>.
- [5] Farajzadeh R, Andrianov A, Zitha PLJ. Investigation of immiscible and miscible foam for enhancing oil recovery. *Ind Eng Chem Res* 2009;49(4):1910–9. <https://doi.org/10.1021/ie901109d>.
- [6] Matthews CS. (1989). Carbon dioxide flooding. In Donaldson, E.C., Chilingarian, G. V., Yen, T.F. (eds.) *Developments in Petroleum Science*, pp. 129-156. Elsevier, Amsterdam. [https://doi.org/10.1016/S0376-7361\(08\)70458-8](https://doi.org/10.1016/S0376-7361(08)70458-8).
- [7] Kuehne DL, Ehman DI, Emanuel AS, Magnani CF. Design and evaluation of a nitrogen-foam field trial. *J Petrol Technol* 1990;42(2):504–12. <https://doi.org/10.2118/17381-PA>.
- [8] Martinsen HA, Vassenden F. Foam-assisted water alternating gas (FAWAG) process on Snorre. *European IOR Symposium*, Brighton, UK 1999. <https://doi.org/10.3997/2214-4609.201406335>.
- [9] Persoff P, Radke CJ, Pruess K, Benson SM, Witherspoon PA. A laboratory investigation of foam flow in sandstone at elevated pressure. *SPE Reservoir Eng* 1991;6(3):365–71.
- [10] Zerhoub M, Touboul E, Ben-Naceur K. Matrix Acidizing: A novel approach to foam diversion. *SPE Annual Technical Conference and Exhibition*, Dallas, TX, USA 1991.
- [11] Kibodeaux KR, Zeilinger SC, Rossen WR. Sensitivity study of foam diversion processes for matrix acidization. *SPE Annual Technical Conference and Exhibition*, New Orleans, Louisiana, USA 1994. <https://doi.org/10.2118/28550-MS>.
- [12] Zeilinger SC, Wang M, Kibodeaux KR, Rossen WR. *Improved Prediction of Foam Diversion in Matrix Acidization*. *SPE Production Operations Symposium*, Oklahoma City, Oklahoma, USA 1995.
- [13] Robert JA, Mack MG. Foam diversion modeling and simulation. *SPE Prod Facil* 1997;12(2):123–8. <https://doi.org/10.2118/29676-PA>.
- [14] Nguyen QP, Currie PK, Zitha PLJ. Determination of Foam Induced Fluid Partitioning in Porous Media using X-ray Computed Tomography. *International Symposium on Oilfield Chemistry*, Houston, Texas, USA 2003.
- [15] Nguyen QP, Zitha PLJ, Currie PK, Rossen WR. CT Study of liquid diversion with foam. *SPE Prod Oper* 2009;24(1):12–21. <https://doi.org/10.2118/93949-PA>.
- [16] Gong J, Vincent Bonnieu S, Kamarul Bahrim RZ, Che Mamat CANB, Groenenboom J, Farajzadeh R, et al. Laboratory investigation of liquid injectivity in surfactant-alternating-gas foam enhanced oil recovery. *Transp Porous Med* 2020;131:85–99. <https://doi.org/10.1007/s11242-018-01231-5>.
- [17] Gong J, Vincent Bonnieu S, Kamarul Bahrim RZ, Che Mamat CANB, Groenenboom J, Farajzadeh R, et al. Modelling of liquid injectivity in surfactant-alternating-gas foam enhanced oil recovery. *SPE J* 2019;24(3):1123–38. <https://doi.org/10.2118/190435-PA>.
- [18] Fredd CN, Fogler HS. Alternative Stimulation Fluids and Their Impact on Carbonate Acidizing. *SPE J* 1998;3(1):34–41. <https://doi.org/10.2118/31074-PA>.
- [19] Osterloh WT, Jante MJ. Effects of gas and liquid velocity on steady-state foam flow at high temperature. *SPE/DOE Symposium on Enhanced Oil Recovery*, Tulsa, Oklahoma, USA 1992.
- [20] Alvarez JM, Rivas HJ, Rossen WR. Unified model for steady-state foam behavior at high and low foam qualities. *SPE J* 2001;6(3):325–33.
- [21] Gong J, Vincent Bonnieu S, Kamarul Bahrim RZ, Che Mamat CANB, Tewari RD, Mahamad Amir MI, et al. Injectivity of multiple gas and liquid slugs in SAG foam EOR: A CT scan study. *SPE J* 2020;25(2):895–906.
- [22] Gong J, Flores Martinez W, Vincent Bonnieu S, Kamarul Bahrim RZ, Che Mamat CANB, Tewari RD, et al. Effect of superficial velocity on liquid injectivity in SAG foam EOR. Part 2: Modelling. Accepted in *Fuel* 2020.